AIAA JOURNAL
Vol. 38, No. 4, April 2000

# Interlaminar Stresses in Laminated Composite Beam-Type Structures Under Shear/Bending

Alberto Milazzo*
*University of Palermo, 90128 Palermo, Italy*

**A boundary integral model for composite laminates under out-of-plane shear/bending is presented. The formulation proposed allows one to determine the elastic response of generally stacked composite laminates having general shape of the cross section. The integral equations governing the ply behavior within the laminate are deduced starting from the reciprocity theorem for beam-type structures. The ply integral equations are obtained by employing the analytical expression of the fundamental solution of generalized plane strain anisotropic problems. The laminate model is completed by imposing the displacement and stress continuity along the interfaces and the external boundary conditions. The formulation is numerically solved by the boundary element method, proposing a solution strategy for standard laminate configurations. The solution of the linear algebraic resolving system provides the displacements and tractions on the boundary of each ply of the laminate. Once this boundary elastic response is known, the displacements and stresses at any internal point of the laminate section are computed using their boundary integral representations. Some applications are presented to demonstrate the accuracy and effectiveness of the method proposed.**

## Nomenclature

| | |
|---|---|
| $\mathcal{D}$, $\mathcal{D}_z$, $\boldsymbol{I}_z$ | = strain operators |
| $\mathcal{D}_n$ | = boundary traction operator |
| $E_{ij}$ | = elasticity stiffness coefficients |
| $\boldsymbol{E}_{1i}$, $\boldsymbol{Q}_i$ | = elasticity matrices |
| $\mathcal{F}$, $\mathcal{G}$ | = shape function matrix |
| $\boldsymbol{f}_j$ | = fundamental solution body forces |
| $m$, $n$ | = number of internal cells and boundary elements |
| $N$ | = number of laminate plies |
| $\boldsymbol{p}$ | = nodal tractions |
| $\boldsymbol{s}$ | = vector of displacements |
| $\boldsymbol{t}$ | = boundary tractions |
| $\boldsymbol{u}$, $\boldsymbol{v}$ | = vector of unknown displacement functions |
| $\boldsymbol{u}_j$, $\boldsymbol{t}_j$ | = fundamental solution displacements and tractions |
| $x_1$, $x_2$, $x_3 \equiv z$ | = coordinate system for the laminate |
| $\alpha_1$, $\alpha_2$ | = boundary normal direction cosines |
| $\beta_{ij}$ | = modified compliances |
| $\Gamma_{\langle k \rangle}$ | = ply section boundary |
| $\gamma$ | = shear/bending loading parameter |
| $\boldsymbol{\delta}$, $\boldsymbol{d}$ | = nodal displacements |
| $\varepsilon$ | = vector of strains |
| $\varepsilon_{ij}$ | = strain components |
| $\boldsymbol{\varepsilon}_j$, $\boldsymbol{\sigma}_j$, $\boldsymbol{\tau}_j$ | = fundamental solution strain and stress vectors |
| $\boldsymbol{\sigma}$, $\boldsymbol{\tau}$ | = stress vectors |
| $\sigma_{ij}$ | = stress components |
| $\Omega_{\langle k \rangle}$ | = ply section domain |

*Subscripts and Superscripts*

| | |
|---|---|
| $(j)$, $(r)$ | = $j$th boundary element and $r$th cell parameters |
| $\langle k \rangle$ | = $k$th ply quantities |
| $u$ | = along laminate axis constant components |
| $v$ | = along laminate axis linearly varying components |

## Introduction

COMPOSITE laminates are widely employed, and they are fundamental members of the lightweight structure technology. The behavior of composite laminates is characterized by complex three-dimensional stress states evidencing high interlaminar stresses caused by the inherent anisotropy and mismatches in the material properties of these structural members.[1] The interlaminar stresses are responsible for the free edge delamination and its growth, which are items of primary concern in composite design. Therefore, the accurate prediction of interlaminar stresses is of capital importance to effectively prevent composite laminate failure. A great deal of research has been carried out to determine and analyze the interlaminar stresses in fiber-reinforced composite laminates, with particular care devoted to their behavior in proximity of free edges. To develop the methods of analysis and provide an insight into the mechanisms governing the laminate elastic response, attention has been focused on the case of interlaminar stresses at the straight edges of laminates under uniaxial loading or pure bending. The first solution of this problem was presented by Pipes and Pagano,[2] who employed the finite difference approach to solve the elasticity governing equations. This solution technique was also employed by other authors to analyze both axial loading and pure bending.[3,4] The finite element method has been extensively used to investigate the problem,[5–12] and many approaches are available that are distinguished one from the other in the kind of elements employed, in the discretization schemes, and in the formulation of the problem. In the literature some methods have also been specifically developed to analyze the composite laminate elastic response. These include boundary-layer theories,[13,14] perturbation techniques,[15] polynomial and Fourier series,[16,17] Lekhnitskii's stress potentials,[18,19] and Reissner's variational principle.[20,21] An important class of solutions was obtained by using the force balance method coupled with the minimization of the complementary energy.[22,23] These methods provide a simple and sufficiently accurate tool for calculating interlaminar stresses. An integral equation representation and solution for composite laminates under axial loading was proposed by Davì and Milazzo,[24–26] who evidenced the accuracy and effectiveness of this approach. Some researchers have presented analyses relative to composite laminates subjected to other loading systems, but these investigations are rather rare. A finite element bending solution was presented by Ye,[27] and Chan and Ochoa[28,29] proposed a quasi-three-dimensional finite element method to investigate composite laminates under tension, bending, and torsion. Bending and torsion solutions were obtained by Yin,[30,31] who used a Lekhnitskii's stress potential approach, by Murthy and Chamis,[32] who employed a three-dimensional finite element model, and by Davì and Milazzo, who proposed a boundary integral formulation for composite laminates in bending[33] and torsion.[34] The out-of-plane shear/bending loading condition is a topic of primary concern in composite structural

Received 30 November 1998; revision received 13 July 1999; accepted for publication 30 August 1999. Copyright © 1999 by the American Institute of Aeronautics and Astronautics, Inc. All rights reserved.

*Research Engineer, Dipartimento di Meccanica e Aeronautica, Viale delle Scienze. Member AIAA.

design particularly for airframe and rotor system structures. Leger and Chan[35] took the out-of-plane shear/bending load condition into account in an approximate fashion. More detailed models for out-of-plane shear/bending were proposed by Murthy and Chamis[32] and Kassapoglou.[36] Finally, Kim and Atluri[37] presented a comprehensive approach for out-of-plane shear/bending of beam-type composite laminate structures. Their solution is based on a variation of the force balance method, which rests on the assumption of an equilibrated stress representation and the use of the principle of minimum complementary energy to determine the elastic response unknown parameters. More recently Davì[38] proposed a general formulation for the analysis of cross-ply laminates under axial load, bending moments, shear/bending, and torsion. The formulation is based on the integral equation theory and is solved by the boundary element method. In the present paper a new formulation based on the integral equation theory is developed for the analysis of the elastic response of general composite laminates subjected to out-of-plane shear/bending loading. The integral equation representation for the problem is directly deduced from the reciprocity theorem for beam-type structures, and it is numerically solved by the boundary element method. Numerical applications are presented to show the accuracy and robustness of the method presented.

## Governing Equations

Consider a beam-type composite laminate referred to a coordinate system $x_1$, $x_2$, $x_3$ with the $x_3 \equiv z$ axis parallel to the generators of the beam lateral surface as shown in Fig. 1. The laminate consists of $N$ anisotropic plies perfectly bonded along the interfaces and with general stacking sequence. Each individual ply has cross section $\Omega_{\langle k\rangle}$ with boundary $\Gamma_{\langle k\rangle} = \Gamma_{e\langle k\rangle} \cup \Gamma_k \cup \Gamma_{k-1}$ (Fig. 1). The laminate is subjected to an out-of-plane shear/bending loading in the $x_2 z$ plane characterized by the loading parameter $\gamma$ representing the bending curvature for unit length, which could be calculated, for example, according to the classical laminate plate theory.[1] Assuming that Saint Venant's principle is satisfied, sufficiently far from the laminate ends the displacement field $\boldsymbol{s}$, associated with the loading just described, can be expressed as[39]

$$\boldsymbol{s} = \boldsymbol{u} + z\boldsymbol{v} + \tfrac{1}{2}z^2\boldsymbol{X}_1\gamma - \tfrac{1}{6}z^3\boldsymbol{X}_2\gamma \tag{1}$$

where the rigid motion terms have been dropped and

$$\boldsymbol{u} = \{u_1(x_1, x_2),\ u_2(x_1, x_2),\ u_3(x_1, x_2)\}^T \tag{2}$$

$$\boldsymbol{v} = \{v_1(x_1, x_2),\ v_2(x_1, x_2),\ v_3(x_1, x_2)\}^T \tag{3}$$

$$\boldsymbol{X}_1 = [0 \quad 0 \quad x_2]^T \tag{4}$$

$$\boldsymbol{X}_2 = [0 \quad 1 \quad 0]^T \tag{5}$$

Introducing the strain operators

$$\mathcal{D} = \begin{bmatrix} \partial/\partial x_1 & 0 & \partial/\partial x_2 & 0 & 0 \\ 0 & \partial/\partial x_2 & \partial/\partial x_1 & 0 & 0 \\ 0 & 0 & 0 & \partial/\partial x_1 & \partial/\partial x_2 \end{bmatrix}^T \tag{6}$$

$$\mathcal{D}_z = \begin{bmatrix} 0 & 0 & 0 \\ 0 & 0 & 0 \\ 0 & 0 & 0 \\ 1 & 0 & 0 \\ 0 & 1 & 0 \end{bmatrix} \frac{\partial}{\partial z} = \boldsymbol{I}_z \frac{\partial}{\partial z} \tag{7}$$

the strain field associated to the displacement system given by Eq. (1) is given by

$$\boldsymbol{\varepsilon} = \begin{Bmatrix} \varepsilon_{11} \\ \varepsilon_{22} \\ \varepsilon_{12} \\ \varepsilon_{13} \\ \varepsilon_{23} \end{Bmatrix} = \mathcal{D}\boldsymbol{s} + \mathcal{D}_z\boldsymbol{s} = \mathcal{D}\boldsymbol{u} + \boldsymbol{I}_z\boldsymbol{v} + z\mathcal{D}\boldsymbol{v} = \boldsymbol{\varepsilon}_u + z\boldsymbol{\varepsilon}_v \tag{8}$$

$$\varepsilon_{33} = v_3 + zx_2\gamma = \varepsilon_{33u} + z\varepsilon_{33v} \tag{9}$$

The subscripts $u$ and $v$ refer to components of the elastic response, which are constant and linearly variable along the $z$ axis, respectively. The stress field in each ply of the laminate is expressed through the generalized Hooke's law. Accounting for the form of the strain field, the constitutive equations can be conveniently written as

$$\begin{Bmatrix} \boldsymbol{\sigma} \\ \hdashline \sigma_{33} \end{Bmatrix} = \begin{Bmatrix} \sigma_{11} \\ \sigma_{22} \\ \sigma_{12} \\ \sigma_{31} \\ \sigma_{32} \\ \hdashline \sigma_{33} \end{Bmatrix} = \left[\begin{array}{ccccc:c} E_{11} & E_{12} & E_{13} & E_{14} & E_{15} & E_{16} \\ E_{12} & E_{22} & E_{23} & E_{24} & E_{25} & E_{26} \\ E_{13} & E_{23} & E_{33} & E_{34} & E_{35} & E_{36} \\ E_{14} & E_{24} & E_{34} & E_{44} & E_{45} & E_{46} \\ E_{15} & E_{25} & E_{35} & E_{45} & E_{55} & E_{56} \\ \hdashline E_{16} & E_{26} & E_{36} & E_{46} & E_{56} & E_{66} \end{array}\right] \begin{Bmatrix} \varepsilon_{11} \\ \varepsilon_{22} \\ \varepsilon_{12} \\ \varepsilon_{31} \\ \varepsilon_{32} \\ \hdashline \varepsilon_{33} \end{Bmatrix}$$

$$= \left[\begin{array}{c:c} \boldsymbol{E}_{11} & \boldsymbol{E}_{12} \\ \hdashline \boldsymbol{E}_{12}^T & E_{66} \end{array}\right] \begin{Bmatrix} \boldsymbol{\varepsilon} \\ \hdashline \varepsilon_{33} \end{Bmatrix} = \begin{Bmatrix} \boldsymbol{\sigma}_u \\ \hdashline \sigma_{33u} \end{Bmatrix} + z \begin{Bmatrix} \boldsymbol{\sigma}_v \\ \hdashline \sigma_{33v} \end{Bmatrix} \tag{10}$$

Again, let us denote

$$\boldsymbol{\tau} = \begin{Bmatrix} \sigma_{31} \\ \sigma_{32} \\ \sigma_{33} \end{Bmatrix} = \left[\begin{array}{ccccc:c} E_{14} & E_{24} & E_{34} & E_{44} & E_{45} & E_{46} \\ E_{15} & E_{25} & E_{35} & E_{45} & E_{55} & E_{56} \\ E_{16} & E_{26} & E_{36} & E_{46} & E_{56} & E_{66} \end{array}\right] \begin{Bmatrix} \varepsilon_{11} \\ \varepsilon_{22} \\ \varepsilon_{12} \\ \varepsilon_{31} \\ \varepsilon_{32} \\ \hdashline \varepsilon_{33} \end{Bmatrix}$$

$$= [\boldsymbol{Q}_1 \,\vdots\, \boldsymbol{Q}_2] \begin{Bmatrix} \boldsymbol{\varepsilon} \\ \hdashline \varepsilon_{33} \end{Bmatrix} = \boldsymbol{\tau}_u + z\boldsymbol{\tau}_v \tag{11}$$

With the notation just introduced the equilibrium equations in $\Omega_{\langle k\rangle}$ are given by

$$\mathcal{D}^T\boldsymbol{\sigma} + \frac{\partial \boldsymbol{\tau}}{\partial z} = \boldsymbol{0} \tag{12}$$

Upon substituting for $\boldsymbol{\sigma}$ and $\boldsymbol{\tau}$ from Eqs. (10) and (11), Eq. (12) gives

$$\mathcal{D}^T\boldsymbol{E}_{11}\mathcal{D}\boldsymbol{u} + \left(\mathcal{D}^T\boldsymbol{Q}_1^T + \boldsymbol{Q}_1\mathcal{D}\right)\boldsymbol{v} + \boldsymbol{Q}_2x_2\gamma$$

$$+ z\left(\mathcal{D}^T\boldsymbol{E}_{11}\mathcal{D}\boldsymbol{v} + \mathcal{D}^T\boldsymbol{E}_{12}x_2\gamma\right) = \boldsymbol{0} \tag{13}$$

Equation (13) is verified to make the following expressions fulfilled simultaneously:

$$\mathcal{D}^T\boldsymbol{E}_{11}\mathcal{D}\boldsymbol{v} + \mathcal{D}^T\boldsymbol{E}_{12}x_2\gamma = \boldsymbol{0} \tag{14}$$

$$\mathcal{D}^T\boldsymbol{E}_{11}\mathcal{D}\boldsymbol{u} + \left(\mathcal{D}^T\boldsymbol{Q}_1^T + \boldsymbol{Q}_1\mathcal{D}\right)\boldsymbol{v} + \boldsymbol{Q}_2x_2\gamma = \boldsymbol{0} \tag{15}$$

Equations (14) and (15) constitute an uncoupled system of partial differential equations, which governs the laminate elastic response

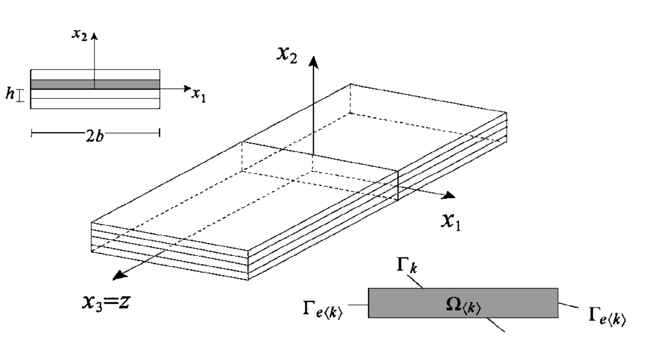


**Fig. 1 Laminate configuration.**

with the appropriate boundary conditions. According to the mathematical structure evidenced by the laminate elastic response, the boundary tractions on $\Gamma_{\langle k\rangle}$ are

$$\boldsymbol{t} = \mathcal{D}_n \boldsymbol{\sigma} = \boldsymbol{t}_u + z\boldsymbol{t}_v \tag{16}$$

where

$$\mathcal{D}_n = \begin{bmatrix} \alpha_1 & 0 & \alpha_2 & 0 & 0 \\ 0 & \alpha_2 & \alpha_1 & 0 & 0 \\ 0 & 0 & 0 & \alpha_1 & \alpha_2 \end{bmatrix} \tag{17}$$

In Eq. (17) $\alpha_1$ and $\alpha_2$ are the direction cosines of the outer normal to the boundary. The mechanical boundary conditions for Eqs. (14) and (15) are therefore supplied in terms of assigned values of the traction functions $\boldsymbol{t}_v$ and $\boldsymbol{t}_u$, respectively, whereas the kinematical boundary conditions are given in terms of prescribed displacement functions $\boldsymbol{v}$ and $\boldsymbol{u}$.

## Integral Equation Representation

For each individual ply within the laminate, let us consider the displacement field $\boldsymbol{u}_j = \boldsymbol{u}_j(x_1, x_2)$ characterizing a solution of the elastic problem. This displacement field, according to the notation introduced, satisfies the relation

$$\mathcal{D}^T \boldsymbol{E}_{11} \mathcal{D} \boldsymbol{u}_j + \boldsymbol{f}_j = \boldsymbol{0} \tag{18}$$

where $\boldsymbol{f}_j = \boldsymbol{f}_j(x_1, x_2)$ is a fictitious system of body forces applied to the ply. Let again $\boldsymbol{\varepsilon}_j$, $\boldsymbol{\sigma}_j$, and $\boldsymbol{t}_j$ be the strains, stresses, and boundary tractions of this solution. Applying the reciprocity theorem for beam-type structures[26] to the particular solution just introduced and the actual elastic response of the ply within the laminate, one obtains

$$\int_{\Gamma_{\langle k\rangle}} \left(\boldsymbol{t}_j^T \boldsymbol{s} - \boldsymbol{u}_j^T \boldsymbol{t}\right) \mathrm{d}\Gamma + \int_{\Omega_{\langle k\rangle}} \boldsymbol{f}_j^T \boldsymbol{s}\, \mathrm{d}\Omega = \int_{\Omega_{\langle k\rangle}} \frac{\partial}{\partial z}\left(\boldsymbol{u}_j^T \boldsymbol{\tau} - \boldsymbol{\tau}_j^T \boldsymbol{s}\right) \mathrm{d}\Omega \tag{19}$$

where $\boldsymbol{\tau}_j = \{\sigma_{31j} \;\; \sigma_{32j} \;\; \sigma_{33j}\}^T$. Upon substituting for $\boldsymbol{s}$ from Eq. (1), the expression of the reciprocity theorem for beam-type structures provides the following set of equations, which have to be fulfilled simultaneously:

$$\int_{\Omega_{\langle k\rangle}} \boldsymbol{f}_j^T \boldsymbol{X}_2 \gamma \, \mathrm{d}\Omega + \int_{\Gamma_{\langle k\rangle}} \boldsymbol{t}_j^T \boldsymbol{X}_2 \gamma \, \mathrm{d}\Omega = 0 \tag{20}$$

$$\int_{\Omega_{\langle k\rangle}} \boldsymbol{f}_j^T \boldsymbol{X}_1 \gamma \, \mathrm{d}\Omega + \int_{\Gamma_{\langle k\rangle}} \boldsymbol{t}_j^T \boldsymbol{X}_1 \gamma \, \mathrm{d}\Omega - \int_{\Omega_{\langle k\rangle}} \boldsymbol{\tau}_j^T \boldsymbol{X}_2 \gamma \, \mathrm{d}\Omega = 0 \tag{21}$$

$$\int_{\Gamma_{\langle k\rangle}} \left(\boldsymbol{t}_j^T \boldsymbol{v} - \boldsymbol{u}_j^T \boldsymbol{t}_v\right) \mathrm{d}\Gamma + \int_{\Omega_{\langle k\rangle}} \boldsymbol{f}_j^T \boldsymbol{v}\, \mathrm{d}\Omega + \int_{\Omega_{\langle k\rangle}} \boldsymbol{\tau}_j^T \boldsymbol{X}_1 \gamma \, \mathrm{d}\Omega = 0 \tag{22}$$

$$\int_{\Gamma_{\langle k\rangle}} \left(\boldsymbol{t}_j^T \boldsymbol{u} - \boldsymbol{u}_j^T \boldsymbol{t}_u\right) \mathrm{d}\Gamma + \int_{\Omega_{\langle k\rangle}} \boldsymbol{f}_j^T \boldsymbol{u}\, \mathrm{d}\Omega + \int_{\Omega_{\langle k\rangle}} \left(\boldsymbol{\tau}_j^T \boldsymbol{v} - \boldsymbol{u}_j^T \boldsymbol{\tau}_v\right) \mathrm{d}\Omega = 0 \tag{23}$$

By using the divergence theorem, one recognizes that Eqs. (20) and (21) are identically satisfied. Therefore the reciprocity theorem for the ply reduces to the two integral relations (22) and (23) only. These integral relations are the basis to derive the integral equation representation employed in the method proposed directly. In fact, let us consider the body forces $\boldsymbol{f}_j$ to be a concentrated load uniformly distributed along a line parallel to the longitudinal axis $z$ and applied in the $j$ direction. Indicating with $P_0$ the load application point in the ply section, the mathematical representation of $\boldsymbol{f}_j$ is given by

$$\boldsymbol{f}_j = \boldsymbol{c}_j \delta(P - P_0) \tag{24}$$

where $\delta$ denotes the Dirac function and $\boldsymbol{c}_j$ is the vector containing the components of the concentrated load. In this case the solution of Eq. (18) represents the singular fundamental solution of the problem. Therefore, through a suitable limit procedure and the use of the divergence theorem, Eqs. (22) and (23) become

$$\boldsymbol{c}_j^T \boldsymbol{v}(P_0) + \int_{\Gamma_{\langle k\rangle}} \left(\boldsymbol{t}_j^T \boldsymbol{v} - \boldsymbol{u}_j^T \boldsymbol{t}_v\right) \mathrm{d}\Gamma + \int_{\Omega_{\langle k\rangle}} \boldsymbol{\varepsilon}_j^T \boldsymbol{E}_{12} x_2 \gamma \, \mathrm{d}\Omega = 0 \tag{25}$$

$$\begin{aligned} \boldsymbol{c}_j^T \boldsymbol{u}(P_0) &+ \int_{\Gamma_{\langle k\rangle}} \left(\boldsymbol{t}_j^T \boldsymbol{u} - \boldsymbol{u}_j^T \boldsymbol{t}_u\right) \mathrm{d}\Gamma - \int_{\Omega_{\langle k\rangle}} \boldsymbol{u}_j^T \left(\mathcal{D}^T \boldsymbol{Q}_1^T + \boldsymbol{Q}_1 \mathcal{D}\right) \boldsymbol{v}\, \mathrm{d}\Omega \\ &+ \int_{\Gamma_{\langle k\rangle}} \boldsymbol{u}_j^T \mathcal{D}_n \boldsymbol{Q}_1^T \boldsymbol{v}\, \mathrm{d}\Gamma - \int_{\Omega_{\langle k\rangle}} \boldsymbol{u}_j^T \boldsymbol{Q}_2 x_2 \gamma \, \mathrm{d}\Omega = 0 \end{aligned} \tag{26}$$

Equations (25) and (26) can be regarded as the form of the beam-type structure Somigliana identity for the ply within the laminate. Indeed they provide a direct link between the displacements functions $\boldsymbol{v}$ and $\boldsymbol{u}$ at the field point $P_0$ and the characteristics of the elastic response, displacements and tractions, on the boundary. Therefore Eqs. (25) and (26) give a boundary integral representation of the displacement field of the ply. Writing the boundary integral representation given by Eqs. (25) and (26) for three independent fundamental solutions, related to three independent load conditions, one obtains the matrix form of the Somigliana identity for beam-type structures giving the three displacement components at $P_0$. One has

$$\boldsymbol{c}^* \boldsymbol{v}(P_0) = \int_{\Gamma_{\langle k\rangle}} \left(\boldsymbol{u}^* \boldsymbol{t}_v - \boldsymbol{t}^* \boldsymbol{v}\right) \mathrm{d}\Gamma - \int_{\Omega_{\langle k\rangle}} \boldsymbol{\varepsilon}^* \boldsymbol{E}_{12} x_2 \gamma \, \mathrm{d}\Omega \tag{27}$$

$$\begin{aligned} \boldsymbol{c}^* \boldsymbol{u}(P_0) &= \int_{\Gamma_{\langle k\rangle}} \left(\boldsymbol{u}^* \boldsymbol{t}_u - \boldsymbol{t}^* \boldsymbol{u}\right) \mathrm{d}\Gamma + \int_{\Omega_{\langle k\rangle}} \boldsymbol{u}^* \left(\mathcal{D}^T \boldsymbol{Q}_1^T + \boldsymbol{Q}_1 \mathcal{D}\right) \boldsymbol{v}\, \mathrm{d}\Omega \\ &- \int_{\Gamma_{\langle k\rangle}} \boldsymbol{u}^* \mathcal{D}_n \boldsymbol{Q}_1^T \boldsymbol{v}\, \mathrm{d}\Gamma + \int_{\Omega_{\langle k\rangle}} \boldsymbol{u}^* \boldsymbol{Q}_2 x_2 \gamma \, \mathrm{d}\Omega \end{aligned} \tag{28}$$

where

$$\boldsymbol{u}^* = [u_{ij}]^T \tag{29}$$

$$\boldsymbol{t}^* = [t_{ij}]^T \tag{30}$$

$$\boldsymbol{\varepsilon}^* = \left[\mathcal{D}\left(\boldsymbol{u}^{*T}\right)\right]^T \tag{31}$$

In the preceding relations $u_{ij}$ and $t_{ij}$ indicate the $i$th component of displacements and tractions of the fundamental solution associated to the load applied along the $j$ direction. For the matrix of the coefficients $\boldsymbol{c}^*$, one has[25]

$$\boldsymbol{c}^* = [c_{ij}]^T = -\int_{\Gamma} \boldsymbol{t}^* \, \mathrm{d}\Gamma \tag{32}$$

Equations (27) and (28) are valid for each point $P_0$ and then, setting $P_0$ on the boundary, they provide a system of integral equations whose solution with appropriate boundary conditions gives the displacements and tractions on the boundary of the ply. Besides, starting from the boundary integral representation given by Eqs. (27) and (28), one can deduce the boundary integral representation for the stress field in terms of the boundary displacements and tractions. Indeed, applying the strain operator $\mathcal{D}$ to Eqs. (27) and (28) and taking into account the constitutive equations in the form of Eq. (10), one obtains the boundary integral representation of the ply stresses,[34] whose expressions are not here given for brevity's sake.

## Fundamental Solutions

The formulation of the boundary integral equations presented in the preceding section requires the knowledge of the fundamental solution of the problem, i.e., a singular solution of Eq. (18) in the unbounded domain. The characteristics of the fundamental solutions for general anisotropic elasticity caused by a uniform distribution of a concentrated load along a line were studied by Kayupov and Kuriyagawa[40] and Mantic and Paris.[41] They provided an expression of the fundamental solution, which is rather cumbersome to implement and involves complex mathematics. For generalized orthotropic media Davì[25] has proposed a suitable form of the fundamental solution for the generalized plane strain problem defined by Eq. (18). For the present approach the fundamental solutions of the problem were expressly obtained by integrating Eq. (18) on the basis of the Lekhnitskii stress potential theory.[39] In the following the fundamental solution is given explicitly for a suitable use in computations. The anisotropic fundamental solutions depend on the roots $\mu = \xi_k \pm i\zeta_k$ $(k = 1, \ldots, 3)$ of the following secular equation:

$$\det\left(\boldsymbol{\theta}^T \boldsymbol{E}_{11} \boldsymbol{\theta}\right) = 0 \tag{33}$$

where

$$\boldsymbol{\theta} = \begin{bmatrix} 1 & 0 & \mu & 0 & 0 \\ 0 & \mu & 1 & 0 & 0 \\ 0 & 0 & 0 & 1 & \mu \end{bmatrix}^T \tag{34}$$

The fundamental solution associated to a load directed along the $j$ direction is characterized by the following displacement field:

$$\boldsymbol{u}_j(P, P_0) = 2\sum_{k=1}^{3} \Re(Q_{kj}\boldsymbol{w}_k)\,\ln R_k - \Im(Q_{kj}\boldsymbol{w}_k)\tan^{-1}\frac{Y_k}{X_k} \tag{35}$$

Let $\boldsymbol{\beta}$ be $\boldsymbol{\beta} = [\beta_{pq}] = \boldsymbol{E}_{11}^{-1}$, in Eq. (35) one has

$$\boldsymbol{w}_k = \begin{Bmatrix} w_{1k} \\ w_{2k} \\ w_{3k} \end{Bmatrix} = \begin{Bmatrix} \beta_{11}\mu_k^2 + \beta_{12} - \beta_{13}\mu_k + \beta_{14}\eta_k\mu_k - \beta_{15}\eta_k \\ \beta_{12}\mu_k + \beta_{22}/\mu_k - \beta_{23} + \beta_{24}\eta_k - \beta_{25}\eta_k/\mu_k \\ \beta_{15}\mu_k + \beta_{25}/\mu_k - \beta_{35} + \beta_{45}\eta_k - \beta_{55}\eta_k/\mu_k \end{Bmatrix} \tag{36}$$

$$\eta_k = -\frac{\beta_{14}\mu_k^3 - (\beta_{15} + \beta_{43})\mu_k^2 + (\beta_{24} + \beta_{53})\mu_k - \beta_{25}}{\beta_{44}\mu_k^2 - 2\beta_{45}\mu_k + \beta_{55}} \tag{37}$$

$$X_k = [x_1(P) - x_1(P_0)] + \xi_k[x_2(P) - x_2(P_0)] \tag{38}$$

$$Y_k = \zeta_k[x_2(P) - x_2(P_0)] \tag{39}$$

$$R_k = \sqrt{X_k^2 + Y_k^2} \tag{40}$$

In the preceding expressions $P$ and $P_0$ denote the observed and the source point, respectively, and the symbols $\Re$ and $\Im$ indicate the real and imaginary part, respectively. The coefficients $Q_{kj} = Q_{kj}^{\Re} + i\,Q_{kj}^{\Im}$ are determined in such a way that the solution, given by Eq. (35), matches the compatibility and equilibrium conditions. This leads to a system of algebraic equations from which the coefficients $Q_{kj}$ are calculated:

$$\boldsymbol{AQ} = \boldsymbol{F} \tag{41}$$

where

$$\boldsymbol{Q} = \left\{Q_{1j}^{\Re} \quad Q_{2j}^{\Re} \quad Q_{3j}^{\Re} \quad Q_{1j}^{\Im} \quad Q_{2j}^{\Im} \quad Q_{3j}^{\Im}\right\}^T \tag{42}$$

$$\boldsymbol{F} = \{0 \quad 0 \quad 0 \quad c_{1j} \quad c_{2j} \quad c_{3j}\}^T \tag{43}$$

The coefficients of the system are

$$A_{lk} = \Im(w_{lk}) \qquad (k, l = 1, \ldots, 3) \tag{44}$$

$$A_{l(k+3)} = \Re(w_{lk}) \qquad (k, l = 1, \ldots, 3) \tag{45}$$

$$A_{4l} = M_{1l}\left[\Re\left(\mu_l^2\right) - \Im(\mu_l)\right] + M_{2l}\left[\Re(\mu_l) + \Im\left(\mu_l^2\right)\right] \qquad (l = 1, \ldots, 6) \tag{46}$$

$$A_{5l} = -M_{1l}\Re(\mu_l) - M_{2l}[\Im(\mu_l) + 1] \qquad (l = 1, \ldots, 6) \tag{47}$$

$$A_{6l} = M_{1l}[\Re(\eta_l\mu_l) - \Im(\eta_l)] + M_{2k}[\Re(\eta_l) + \Im(\eta_l\mu_l)] \qquad (l = 1, \ldots, 6) \tag{48}$$

where $\mu_{k+3} = \mu_k$ and $\eta_{k+3} = \eta_k$. The coefficients in the preceding equations are given as

$$M_{1k} = -M_{2(k+3)} = -2\pi\frac{\left[\xi_k^2 - \zeta_k^2 + 1 + \zeta_k\left(\xi_k^2 + \zeta_k^2 - 1\right)\right]}{\xi_k^4 + 2\xi_k^2\left(\zeta_k^2 + 1\right) + \zeta_k^4 - 2\zeta_k^2 + 1} \qquad (k = 1, \ldots, 3) \tag{49}$$

$$M_{2k} = M_{1(k+3)} = -2\pi\frac{\xi_k\left(2\zeta_k - \xi_k^2 - \zeta_k^2 - 1\right)}{\xi_k^4 + 2\xi_k^2\left(\zeta_k^2 + 1\right) + \zeta_k^4 - 2\zeta_k^2 + 1} \qquad (k = 1, \ldots, 3) \tag{50}$$

The fundamental solution tractions are obtained from

$$\boldsymbol{t}_j(P, P_0) = 2\sum_{k=1}^{3}\left\{\left(\Re(Q_{kj}\boldsymbol{m}_k)\alpha_1 - \Re\left(Q_{kj}\frac{\boldsymbol{m}_k}{\mu_k}\right)\alpha_2\right)\frac{X_k}{R_k^2} + \left(\Im(Q_{kj}\boldsymbol{m}_k)\alpha_1 - \Im\left(Q_{kj}\frac{\boldsymbol{m}_k}{\mu_k}\right)\alpha_2\right)\frac{Y_k}{R_k^2}\right\} \tag{51}$$

where

$$\boldsymbol{m}_k = \left\{\mu_k^2,\ \mu_k,\ \mu_k\eta_k\right\}^T \tag{52}$$

In general the three independent fundamental solutions employed for the outlining of the formulation are obtained by setting $c_{ij} = \delta_{ij}$, where $\delta_{ij}$ is the Kronecker delta. By so doing when $P_0$ lies on a regular boundary the fundamental solution chosen provides $c_{ij} = \frac{1}{2}\delta_{ij}$. The kernels needed for the calculation of the internal stress field can be found by applying the strain operator $\mathcal{D}$ to the displacement and traction kernels. In the common case of plies characterized by a generalized orthotropic law, the expressions of the fundamental solutions simplify and reduce to the form given in Refs. 25, 26, and 34.

## Boundary Element Model

Following the classical approach for solving boundary problems, the solution of the formulation proposed is obtained by discretizing the boundary $\Gamma_{\langle k\rangle}$ of each ply into $n$ boundary elements and the domain $\Omega_{\langle k\rangle}$ into $m$ internal cells with domain $\Omega_r$. On each boundary element $\Gamma_j$ the displacement function $\boldsymbol{v}$ and the tractions $\boldsymbol{t}_v$ are expressed by using their nodal values $\boldsymbol{\delta}_v^{(j)}$ and $\boldsymbol{p}_v^{(j)}$ through suitable shape functions $\mathcal{F}(s)$:

$$\boldsymbol{v} = \mathcal{F}\boldsymbol{\delta}_v^{(j)} \tag{53}$$

$$\boldsymbol{t}_v = \mathcal{F}\boldsymbol{p}_v^{(j)} \tag{54}$$

With these assumptions the discretized version of Eq. (27) for any point $P_i$ is

$$\boldsymbol{c}^*\boldsymbol{v}(P_i) + \sum_{j=1}^{n}\hat{\boldsymbol{H}}_{ij}\boldsymbol{\delta}_v^{(j)} + \sum_{j=1}^{n}\boldsymbol{G}_{ij}\boldsymbol{p}_v^{(j)} = \sum_{r=1}^{m}\boldsymbol{B}_{ir} \tag{55}$$

where the influence coefficients and the right-hand side are defined by

$$\hat{\boldsymbol{H}}_{ij} = \int_{\Gamma_j}\boldsymbol{t}^*(P, P_i)\,\mathcal{F}(P)\,\mathrm{d}\Gamma \tag{56}$$

$$\boldsymbol{G}_{ij} = -\int_{\Gamma_j}\boldsymbol{u}^*(P, P_i)\,\mathcal{F}(P)\,\mathrm{d}\Gamma \tag{57}$$

$$\boldsymbol{B}_{ir} = \int_{\Omega_r}\varepsilon^*(P, P_i)\boldsymbol{E}_{12}x_2\gamma\,\mathrm{d}\Omega \tag{58}$$

Analogously on the boundary element $\Gamma_j$ the displacement functions $\boldsymbol{u}$ and the tractions $\boldsymbol{t}_u$ are expressed in terms of their boundary nodal values $\boldsymbol{\delta}_u^{(j)}$ and $\boldsymbol{p}_u^{(j)}$. One has

$$\boldsymbol{u} = \mathcal{F}\boldsymbol{\delta}_u^{(j)} \tag{59}$$

$$\boldsymbol{t}_u = \mathcal{F}\boldsymbol{p}_u^{(j)} \tag{60}$$

Moreover let us assume that on the $r$th cell the displacement function $\boldsymbol{v}$ can be interpolated as

$$\boldsymbol{v} = \mathcal{G}\boldsymbol{d}_v^{(r)} \tag{61}$$

where $\boldsymbol{d}_v^{(r)}$ is the vector collecting the cell nodal values of $\boldsymbol{v}$ and $\mathcal{G}(s_1, s_2)$ is a suitable matrix of shape functions. The discretized version of Eq. (28) is

$$\boldsymbol{c}^*\boldsymbol{u}(P_i) + \sum_{j=1}^{n}\hat{\boldsymbol{H}}_{ij}\boldsymbol{\delta}_u^{(j)} + \sum_{j=1}^{n}\boldsymbol{G}_{ij}\boldsymbol{p}_u^{(j)} = \sum_{j=1}^{n}\boldsymbol{J}_{ij}\boldsymbol{\delta}_v^{(j)} + \sum_{r=1}^{m}\boldsymbol{W}_{ir}\boldsymbol{d}_v^{(r)} + \sum_{r=1}^{m}\boldsymbol{Y}_{ir} \tag{62}$$

where

$$\boldsymbol{J}_{ij} = -\int_{\Gamma_j} \boldsymbol{u}^*(P, P_i)\mathcal{D}_n\boldsymbol{Q}_1^T\mathcal{F}(P)\,\mathrm{d}\Gamma \tag{63}$$

$$\boldsymbol{W}_{ir} = \int_{\Omega_r} \boldsymbol{u}^*(P, P_i)\left(\mathcal{D}^T\boldsymbol{Q}_1^T + \boldsymbol{Q}_1\mathcal{D}\right)\mathcal{G}(P)\,\mathrm{d}\Omega \tag{64}$$

$$\boldsymbol{Y}_{ir} = \int_{\Omega_r} \boldsymbol{u}^*(P, P_i)\boldsymbol{Q}_2 x_2 \gamma\,\mathrm{d}\Omega \tag{65}$$

The boundary discretized model governing the behavior of the $k$th ply within the laminate is obtained by collocating Eqs. (55) and (62) at the boundary nodes and taking into account the relation between the cell nodal values of $\boldsymbol{v}$ and the boundary nodal values of $\boldsymbol{v}$ and $\boldsymbol{t}_v$, i.e., Eq. (55). By so doing one obtains

$$\boldsymbol{H}_{\langle k\rangle}\boldsymbol{\delta}_{v\langle k\rangle} + \boldsymbol{G}_{\langle k\rangle}\boldsymbol{p}_{v\langle k\rangle} = \boldsymbol{B}_{\langle k\rangle} \tag{66}$$

$$\boldsymbol{H}_{\langle k\rangle}\boldsymbol{\delta}_{u\langle k\rangle} + \boldsymbol{G}_{\langle k\rangle}\boldsymbol{p}_{u\langle k\rangle} = \boldsymbol{J}_{\langle k\rangle}\boldsymbol{\delta}_{v\langle k\rangle} + \boldsymbol{W}_{\langle k\rangle}\boldsymbol{d}_{v\langle k\rangle} + \boldsymbol{Y}_{\langle k\rangle} \tag{67}$$

$$\boldsymbol{d}_{v\langle k\rangle} = \bar{\boldsymbol{H}}_{\langle k\rangle}\boldsymbol{\delta}_{v\langle k\rangle} + \bar{\boldsymbol{G}}_{\langle k\rangle}\boldsymbol{p}_{v\langle k\rangle} + \bar{\boldsymbol{B}}_{\langle k\rangle} \tag{68}$$

where $\boldsymbol{\delta}_{v\langle k\rangle}$ and $\boldsymbol{\delta}_{u\langle k\rangle}$ contain the boundary nodal values of the displacements $\boldsymbol{v}$ and $\boldsymbol{u}$, $\boldsymbol{p}_{v\langle k\rangle}$ and $\boldsymbol{p}_{u\langle k\rangle}$ contain the nodal values of the boundary tractions $\boldsymbol{t}_v$ and $\boldsymbol{t}_u$, and $\boldsymbol{d}_v$ is the vector of the nodal displacements $\boldsymbol{v}$. The notation $\langle k\rangle$ denotes quantities referred to the $k$th ply. The boundary element model for the whole laminate is directly deduced starting from the model obtained for the individual ply. The resolving system for the laminate problem is obtained by writing the integral equation model for all of the plies of the laminate and imposing the interface continuity conditions and the external boundary conditions. The solution strategy of the discretized model is based on the uncoupling of the equations constituting the resolving system. Indeed, upon substituting Eq. (68) into Eq. (66), one obtains the laminate resolving system in the following form ($k = 1, 2, \ldots, N$):

$$\boldsymbol{H}_{\langle k\rangle}\boldsymbol{\delta}_{v\langle k\rangle} + \boldsymbol{G}_{\langle k\rangle}\boldsymbol{p}_{v\langle k\rangle} = \boldsymbol{B}_{\langle k\rangle} \tag{69}$$

$$\begin{aligned}\boldsymbol{H}_{\langle k\rangle}\boldsymbol{\delta}_{u\langle k\rangle} + \boldsymbol{G}_{\langle k\rangle}\boldsymbol{p}_{u\langle k\rangle} &= \left(\boldsymbol{J}_{\langle k\rangle} + \boldsymbol{W}_{\langle k\rangle}\bar{\boldsymbol{H}}_{\langle k\rangle}\right)\boldsymbol{\delta}_{v\langle k\rangle} \\ &\quad + \boldsymbol{W}_{\langle k\rangle}\bar{\boldsymbol{G}}_{\langle k\rangle}\boldsymbol{p}_{v\langle k\rangle} + \boldsymbol{W}_{\langle k\rangle}\bar{\boldsymbol{B}}_{\langle k\rangle} + \boldsymbol{Y}_{\langle k\rangle}\end{aligned} \tag{70}$$

The interface continuity conditions and external boundary conditions need to be added to Eqs. (69) and (70). Let us introduce a partition of the linear algebraic system given by Eqs. (69) and (70) in such a way that the generic vector $\boldsymbol{y}_{\langle k\rangle}$ can be written as

$$\boldsymbol{y}_{\langle k\rangle}^T = \left\{\boldsymbol{y}_{\langle k\rangle}^{\Gamma_{e\langle k\rangle}} \quad \boldsymbol{y}_{\langle k\rangle}^{\Gamma_{k-1}} \quad \boldsymbol{y}_{\langle k\rangle}^{\Gamma_k}\right\} \tag{71}$$

where the vectors $\boldsymbol{y}_{\langle k\rangle}^{\Gamma_{k-1}}$ and $\boldsymbol{y}_{\langle k\rangle}^{\Gamma_k}$ collect the components of $\boldsymbol{y}_{\langle k\rangle}$ associated with the nodes belonging to the interfaces $\Gamma_{k-1}$ and $\Gamma_k$ and the vector $\boldsymbol{y}_{\langle k\rangle}^{\Gamma_{e\langle k\rangle}}$ contains the components of $\boldsymbol{y}_{\langle k\rangle}$ associated with the nodes lying on the external boundary $\Gamma_{e\langle k\rangle}$ (see Fig. 1). By so doing the interface continuity conditions in the discretized model are given by ($k = 1, 2, \ldots, N - 1$)

$$\boldsymbol{\delta}_{v\langle k\rangle}^{\Gamma_k} = \boldsymbol{\delta}_{v\langle k+1\rangle}^{\Gamma_k} \tag{72}$$

$$\boldsymbol{\delta}_{u\langle k\rangle}^{\Gamma_k} = \boldsymbol{\delta}_{u\langle k+1\rangle}^{\Gamma_k} \tag{73}$$

$$\boldsymbol{p}_{v\langle k\rangle}^{\Gamma_k} = -\boldsymbol{p}_{v\langle k+1\rangle}^{\Gamma_k} \tag{74}$$

$$\boldsymbol{p}_{u\langle k\rangle}^{\Gamma_k} = -\boldsymbol{p}_{u\langle k+1\rangle}^{\Gamma_k} \tag{75}$$

and the external boundary conditions are expressed by ($k = 1, 2, \ldots, N$)

$$\boldsymbol{p}_{v\langle k\rangle}^{\Gamma_{e\langle k\rangle}} = \boldsymbol{0} \tag{76}$$

$$\boldsymbol{p}_{u\langle k\rangle}^{\Gamma_{e\langle k\rangle}} = \boldsymbol{0} \tag{77}$$

The system of Eqs. (69) and (70), together with the interface continuity conditions Eqs. (72–75) and external boundary conditions Eqs. (76) and (77), evidences the boundary nature of the model from the involvement of boundary unknowns only. Moreover the mathematical structure of the resolving system allows one to uncouple the two equations (69) and (70) with their relative interface continuity and boundary conditions. Therefore the model solution is obtained by solving first for $\boldsymbol{v}$ and $\boldsymbol{p}_v$ and then, upon substituting in Eq. (70), solving for $\boldsymbol{u}$ and $\boldsymbol{p}_u$. Once the boundary solution is known in terms of displacement functions $\boldsymbol{v}$ and $\boldsymbol{u}$ and tractions $\boldsymbol{p}_v$ and $\boldsymbol{p}_u$, the stress field is calculated in a pointwise fashion by using the discretized version of the boundary integral representation for the stresses.[34]

## Solution Strategy

To solve the model for $\boldsymbol{v}$ and $\boldsymbol{p}_v$, the following scheme can be employed. On the basis of the partition introduced in the preceding section, the resolving system for the displacement function $\boldsymbol{v}$ and tractions $\boldsymbol{p}_v$ is

$$\begin{aligned}&\boldsymbol{H}_{\langle k\rangle}^{\Gamma_{e\langle k\rangle}}\boldsymbol{\delta}_{v\langle k\rangle}^{\Gamma_{e\langle k\rangle}} + \boldsymbol{H}_{\langle k\rangle}^{\Gamma_{k-1}}\boldsymbol{\delta}_{v\langle k\rangle}^{\Gamma_{k-1}} + \boldsymbol{H}_{\langle k\rangle}^{\Gamma_k}\boldsymbol{\delta}_{v\langle k\rangle}^{\Gamma_k} \\ &\quad + \boldsymbol{G}_{\langle k\rangle}^{\Gamma_{k-1}}\boldsymbol{p}_{v\langle k\rangle}^{\Gamma_{k-1}} + \boldsymbol{G}_{\langle k\rangle}^{\Gamma_k}\boldsymbol{p}_{v\langle k\rangle}^{\Gamma_k} = \boldsymbol{B}_{\langle k\rangle}, \qquad k = 1, \ldots, N\end{aligned} \tag{78}$$

$$\boldsymbol{\delta}_{v\langle k\rangle}^{\Gamma_k} = \boldsymbol{\delta}_{v\langle k+1\rangle}^{\Gamma_k}, \qquad k = 1, \ldots, N-1 \tag{79}$$

$$\boldsymbol{p}_{v\langle k\rangle}^{\Gamma_k} = -\boldsymbol{p}_{v\langle k+1\rangle}^{\Gamma_k}, \qquad k = 1, \ldots, N-1 \tag{80}$$

where the boundary conditions given by Eq. (76) have been taken into account. The system of Eqs. (78–80) describes the behavior of each ply within the laminate if one assumes that all of the matrices in which a superscript or subscript $i < 1$ or $i > N$ appears need to be dropped. From Eqs. (78–80), assuming that the displacements $\boldsymbol{\delta}_{v\langle k\rangle}^{\Gamma_{k-1}}$ are known, one deduces

$$\begin{Bmatrix}\boldsymbol{\delta}_{v\langle k\rangle}^{\Gamma_{e\langle k\rangle}} \\ \boldsymbol{\delta}_{v\langle k\rangle}^{\Gamma_k} \\ \boldsymbol{p}_{v\langle k\rangle}^{\Gamma_{k-1}}\end{Bmatrix} = \begin{bmatrix}\boldsymbol{C}_{\langle k\rangle}^{\Gamma_{e\langle k\rangle}} \\ \boldsymbol{C}_{\langle k\rangle}^{\Gamma_k} \\ \boldsymbol{C}_{\langle k\rangle}^{\Gamma_{k-1}}\end{bmatrix}\boldsymbol{p}_{v\langle k\rangle}^{\Gamma_k} + \begin{Bmatrix}\boldsymbol{F}_{v\langle k\rangle}^{\Gamma_{e\langle k\rangle}} \\ \boldsymbol{F}_{v\langle k\rangle}^{\Gamma_k} \\ \boldsymbol{F}_{v\langle k\rangle}^{\Gamma_{k-1}}\end{Bmatrix} = \boldsymbol{C}_{\langle k\rangle}\boldsymbol{p}_{v\langle k\rangle}^{\Gamma_k} + \boldsymbol{F}_{v\langle k\rangle} \tag{81}$$

and then using again Eqs. (78–80) written for the $k+1$ ply, one has

$$\begin{aligned}\begin{Bmatrix}\boldsymbol{\delta}_{v\langle k+1\rangle}^{\Gamma_{e\langle k+1\rangle}} \\ \boldsymbol{\delta}_{v\langle k+1\rangle}^{\Gamma_{k+1}} \\ \boldsymbol{p}_{v\langle k+1\rangle}^{\Gamma_k}\end{Bmatrix} &= \left[\boldsymbol{H}_{\langle k+1\rangle}^{\Gamma_{e\langle k+1\rangle}}\boldsymbol{H}_{\langle k+1\rangle}^{\Gamma_{k+1}}\left(\boldsymbol{G}_{\langle k+1\rangle}^{\Gamma_k} - \boldsymbol{H}_{\langle k+1\rangle}^{\Gamma_k}\boldsymbol{C}_{\langle k\rangle}^{\Gamma_k}\right)\right]^{-1} \\ &\quad \times\left(\boldsymbol{B}_{\langle k+1\rangle} - \boldsymbol{H}_{\langle k+1\rangle}^{\Gamma_k}\boldsymbol{F}_{v\langle k\rangle}^{\Gamma_k} - \boldsymbol{G}_{\langle k+1\rangle}^{\Gamma_{k+1}}\boldsymbol{p}_{v\langle k+1\rangle}^{\Gamma_{k+1}}\right) \\ &= \boldsymbol{C}_{\langle k+1\rangle}\boldsymbol{p}_{v\langle k+1\rangle}^{\Gamma_{k+1}} + \boldsymbol{F}_{v\langle k+1\rangle}\end{aligned} \tag{82}$$

Equation (82) is valid for each ply, and it allows one to obtain the expression for $\boldsymbol{C}_{\langle k\rangle}$ and $\boldsymbol{F}_{v\langle k\rangle}$, which are given by

$$\boldsymbol{C}_{\langle k\rangle} = -\Phi_{\langle k\rangle}\boldsymbol{G}_{\langle k\rangle}^{\Gamma_k} \tag{83}$$

$$\boldsymbol{F}_{v\langle k\rangle} = \Phi_{\langle k\rangle}\left(\boldsymbol{B}_{\langle k\rangle} - \boldsymbol{H}_{\langle k\rangle}^{\Gamma_{k-1}}\boldsymbol{F}_{v\langle k-1\rangle}^{\Gamma_{k-1}}\right) \tag{84}$$

where

$$\Phi_{\langle k\rangle} = \left[\boldsymbol{H}_{\langle k\rangle}^{\Gamma_{e\langle k\rangle}}\boldsymbol{H}_{\langle k\rangle}^{\Gamma_k}\left(\boldsymbol{G}_{\langle k\rangle}^{\Gamma_{k-1}} - \boldsymbol{H}_{\langle k\rangle}^{\Gamma_{k-1}}\boldsymbol{C}_{\langle k-1\rangle}^{\Gamma_{k-1}}\right)\right]^{-1} \tag{85}$$

Therefore, by applying recursively the expression (82), one determines $\boldsymbol{v}$ and $\boldsymbol{p}_v$. By using the same solution scheme for the second part of the resolving system, one can calculate $\boldsymbol{\delta}_{u\langle k\rangle}$ and $\boldsymbol{p}_{u\langle k\rangle}$. In this case the solution is given by

$$\begin{Bmatrix}\boldsymbol{\delta}_{u\langle k\rangle}^{\Gamma_{e\langle k\rangle}} \\ \boldsymbol{\delta}_{u\langle k\rangle}^{\Gamma_k} \\ \boldsymbol{p}_{u\langle k\rangle}^{\Gamma_{k-1}}\end{Bmatrix} = \boldsymbol{C}_{\langle k\rangle}\boldsymbol{p}_{u\langle k\rangle}^{\Gamma_k} + \boldsymbol{F}_{u\langle k\rangle} \tag{86}$$

where

$$\begin{aligned}\boldsymbol{F}_{u\langle k\rangle} &= \Phi_{\langle k\rangle}\Big[\left(\boldsymbol{J}_{\langle k\rangle} + \boldsymbol{W}_{\langle k\rangle}\bar{\boldsymbol{H}}_{\langle k\rangle}\right)\boldsymbol{\delta}_{v\langle k\rangle} + \boldsymbol{W}_{\langle k\rangle}\bar{\boldsymbol{G}}_{\langle k\rangle}\boldsymbol{p}_{v\langle k\rangle} \\ &\quad + \boldsymbol{W}_{\langle k\rangle}\bar{\boldsymbol{B}}_{\langle k\rangle} + \boldsymbol{Y}_{\langle k\rangle} - \boldsymbol{H}_{\langle k\rangle}^{\Gamma_{k-1}}\boldsymbol{F}_{u\langle k-1\rangle}^{\Gamma_{k-1}}\Big]\end{aligned} \tag{87}$$

## Numerical Remarks and Applications

The boundary integral equation approach developed in this paper was implemented in a computer code to perform laminate analyses and test the soundness of the formulation. The computer code was implemented assuming straight boundary elements with linear interpolation of the unknown data. For the domain discretization needed to evaluate the domain integrals, four node quadrilateral isoparametric elements are employed. The implementation is centered on the calculation of the influence coefficients through the Gaussian quadrature formulas. An adaptive integration scheme is used with the aim to inherently take into account the kernel singular behavior and set correctly the order of the integration formula employed. The domain integrals that do not depend on the displacement functions are computed after they have been converted into boundary integrals. The technique employed to perform this conversion is the particular solution method.[34,38] The solution of the resolving system is based on the algorithm discussed in the preceding section. The code can handle laminates with general stacking sequence and section geometry exploiting possible symmetries of the system with respect to the coordinate axes. The code allows the calculation of displacements and stresses at internal points through the discretized form of their integral representations. Also in this case Gaussian quadrature formulas are employed in the calculation.

Some applications have been performed to check the accuracy and the effectiveness of the present method and to assess the robustness of the analysis tool in which it has been implemented. The method has been applied to analyze the two cross-ply configurations $[0/90]_s$ and $[90/0]_s$ and the angle-ply laminate $[45/-45]_s$, and the results obtained are discussed in this section. The ply material properties used in the analysis correspond to graphite/epoxy fiber-reinforced laminas.[25] The plies have been considered as having rectangular cross section with thickness $h$ and width $2b = 16h$. The discretization employed for each individual ply is shown in Fig. 2, where the boundary elements and the internal nodes are recorded. The first analysis presented is relative to the cross-ply configurations. Figures 3 and 4 show the interlaminar stress distributions along the semichord ($x_1 > 0$) at the top interface of the laminate. Because of

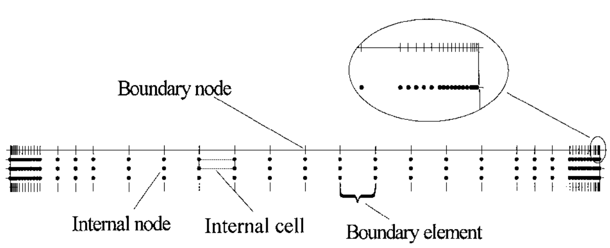


**Fig. 2 Ply discretization.**

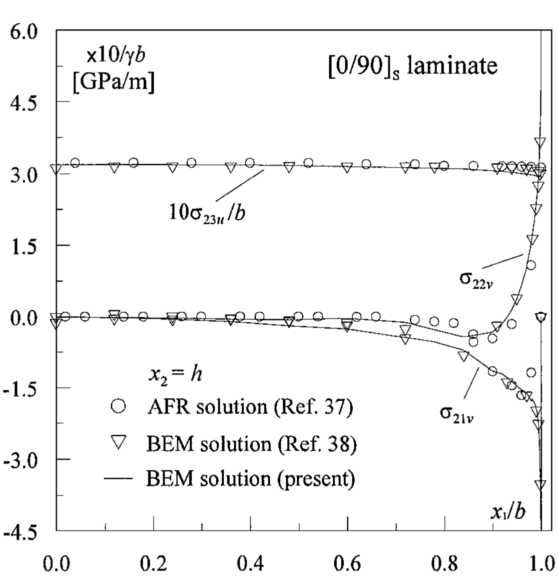


**Fig. 3 Through-width stress distribution for the $[0/90]_s$ laminate under shear/bending loading.**

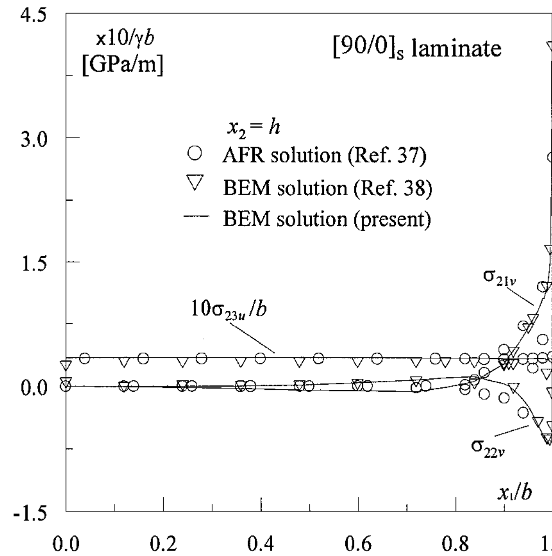


**Fig. 4 Through-width stress distribution for the [90⊲0]$_s$ laminate under shear/bending loading.**

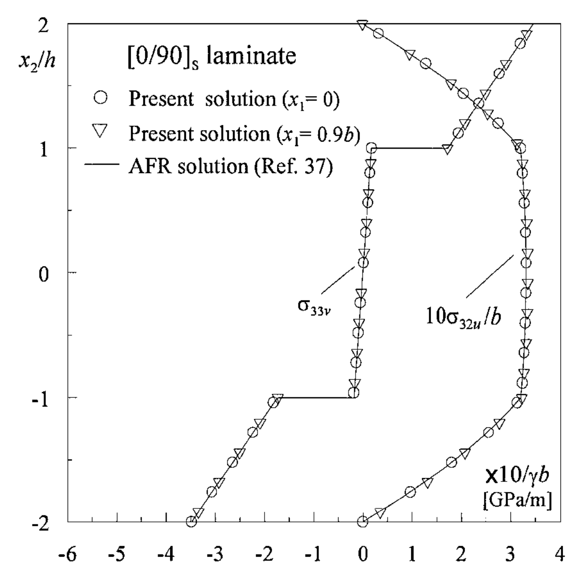


**Fig. 5 Through-thickness stress distribution for the $[0/90]_s$ laminate under shear/bending loading.**

the absence of the in-plane shear stress $\sigma_{31}$, the interlaminar stresses $\sigma_{22}$ and $\sigma_{23}$ exhibit a complete symmetry about the vertical middle plane $x_2\,x_3$, whereas the interlaminar stress $\sigma_{21}$ has a complete antisymmetry. The results shown in Figs. 3 and 4 were obtained without exploiting any structural symmetry, and they are compared to the solution of a different boundary integral model[38] and the solution obtained by using the approach proposed in Ref. 36, which is based upon the admissible function representation method (AFR). The comparison highlights a good agreement among the solutions, and this confirms the features of the present method, which seems to assess very accurately the steep stress gradients near the free edge where a singular behavior of the stress field is expected. Figures 5 and 6 show the through-thickness variations of the interlaminar stresses $\sigma_{32}$ and of the in-plane stress $\sigma_{33}$ for the two cross-ply laminates considered. The through-thickness stress distributions are plotted for two different values of the abscissa $x_1$. The stress patterns are practically coincident as expected because of the nature of cross-ply laminate elastic response. Also in this case the comparison proves the aptitude of the present approach in modeling efficiently the laminate elastic response under shear/bending loads.

The next group of figures, Figs. 7–9, represents the interlaminar stresses for the $[45/-45]_s$ stacking sequence at the top interface over the entire width of the laminate. Once again the comparison of the present solution with the results obtained by applying the admissible

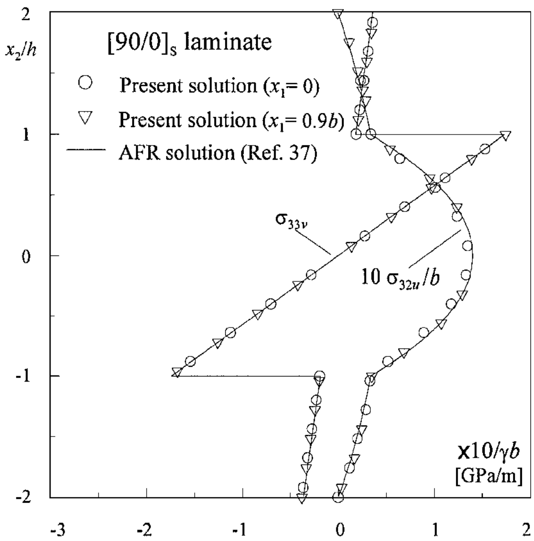


**Fig. 6 Through-thickness stress distribution for the $[90/0]_s$ laminate under shear/bending loading.**

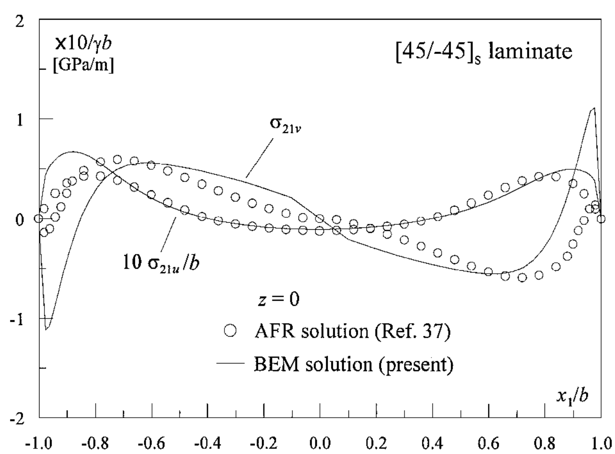


**Fig. 7 The $\sigma_{21}$ through-width distribution for the $[45/-45]_s$ laminate under shear/bending loading.**

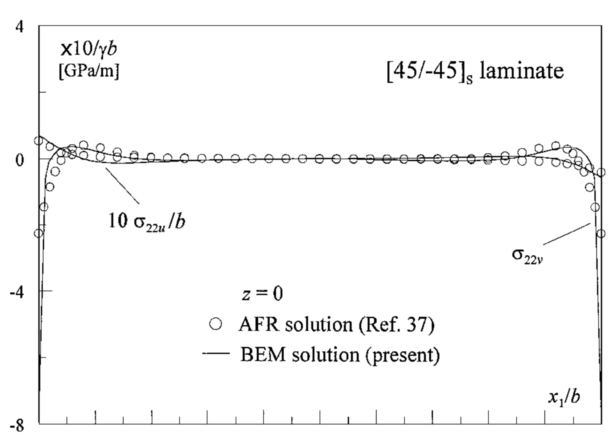


**Fig. 8 The $\sigma_{22}$ through-width distribution for the $[45/-45]_s$ laminate under shear/bending loading.**

function representation method[37] shows a satisfactory agreement. The $[45/-45]_s$ stacking sequence is characterized by high in-plane stress $\sigma_{31}$, which affects the interlaminar stress arrangement with its gradients. As a consequence, all of the symmetries and antisymmetries in the stress patterns break down. This circumstance can be inferred from Figs. 7–9 where the constant and linearly variable components of interlaminar stresses are shown. Moreover, the stress patterns show that the $\sigma_{23}$ stress is an order of magnitude greater

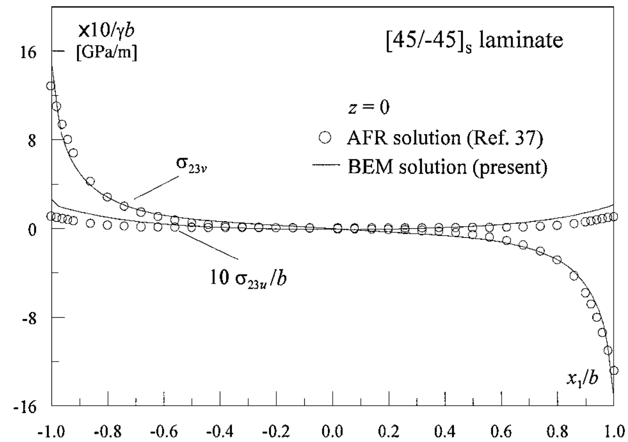


**Fig. 9 The $\sigma_{23}$ through-width distribution for the $[45/-45]_s$ laminate under shear/bending loading.**

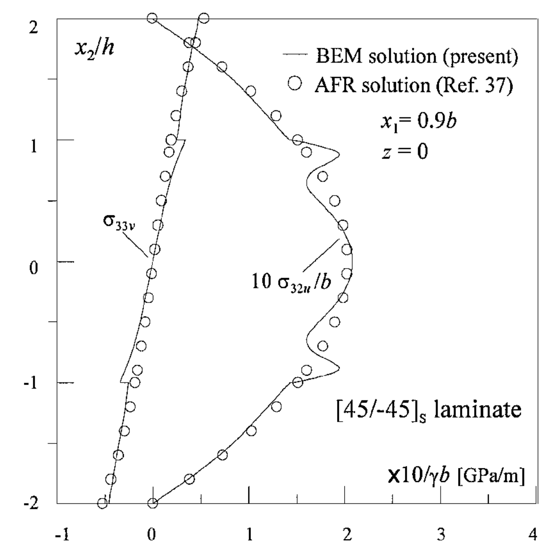


**Fig. 10 Through-thickness stress distribution at $x_1 = 0.9b$ for the $[45/-45]_s$ laminate under shear/bending loading.**

than the other interlaminar stress, and it exhibits very high peaks at the free edge where a singular behavior is then expected. Obviously the unbalanced distribution of $\sigma_{23}$ is more evident in the sections near $z = 0$. The through-thickness variation of stresses was investigated also for the $[45/-45]_s$ angle-ply laminate. The results are presented in Fig. 10, where the $\sigma_{32}$ and $\sigma_{33}$ stresses are plotted.

In conclusion, the results obtained show the accuracy of the present method, which by virtue of its features is able to predict properly the interlaminar stress behavior near the free edge. Near the free edges the stress distributions in both cross-ply and angle-ply laminates under shear/bending experience similar shape and behavior of the stress distribution under axial load or pure bending. However, the out-of-plane loadings represent a very hard condition because it results in higher interlaminar normal and shear stresses than those arising from the other load conditions. This circumstance occurs because the shear/bending load directly subjects the laminate to interlaminar stresses as emphasized by Kim and Atluri.[37]

## Conclusions

A boundary integral representation for the elasticity solution of multilayered, beam-type composite laminates under out-of-plane shear/bending is presented. The problem is exactly formulated, and in the approach all of the elasticity relations, boundary conditions, and interface continuity conditions are strictly satisfied. The numerical solution of the model is achieved through the boundary element method. An efficient solution algorithm is also proposed to benefit from all of the computational advantages of a boundary integral representation. The boundary element solution is numerically consistent, and its accuracy depends on the mesh refinement only because all of the elasticity relations have been exactly satisfied in formulating the problem. The present formulation is an interesting approach to the laminate problem from both a theoretical and a numerical point of view. It allows one to obtain accurate laminate solutions using the well-known computational and theoretical features of boundary integral modelization. Four-ply, symmetric laminates subjected to out-of-plane shear/bending loads have been investigated, and the results obtained compare well with those obtained by using other approaches when the latter are available. The stress patterns obtained near the free edge by using rather coarse meshes highlight the efficacy and the robustness of the method. In conclusion, the present formulation contributes to the outline of the approaches available to analyze composite laminates by providing an efficient and sound method to investigate accurately the behavior of general composite laminates under out-of-plane shear/bending.

## Acknowledgment

The author is grateful to G. Davì for his encouragement and kind assistance throughout the work described in this paper.

## References

[1]Jones, R. M., *Mechanics of Composite Materials*, Hemisphere, New York, 1975.

[2]Pipes, R. B., and Pagano, N. J., "Interlaminar Stresses in Composite Laminates Under Uniform Axial Extension," *Journal of Composite Materials*, Vol. 4, Oct. 1970, pp. 538–548.

[3]Altus, E., Rotem, A., and Shmueli, M., "Free Edge Effect in Angle-Ply Laminates—A New Three Dimensional Finite Difference Solution," *Journal of Composite Materials*, Vol. 14, Jan. 1980, pp. 21–30.

[4]Salamon, N. J., "Interlaminar Stresses in Layered Composite Laminates in Bending," *Journal of Fiber Science and Technology*, Vol. 2, No. 3, 1978, pp. 305–317.

[5]Rybicki, E. F., "Approximate Three-Dimensional Solutions for Symmetric Laminates Under Inplane Loading," *Journal of Composite Materials*, Vol. 5, July 1971, pp. 354–360.

[6]Wang, A. S. D., and Crossman, F. W., "Some New Results on Edge Effect in Symmetric Composite Laminates," *Journal of Composite Materials*, Vol. 11, Jan. 1977, pp. 92–106.

[7]Spilker, R. L., and Chou, S. C., "Edge Effect in Symmetric Composite Laminates: Importance of Satisfying the Traction Free Edge," *Journal of Composite Materials*, Vol. 14, Jan. 1980, pp. 2–19.

[8]Wang, S. S., and Stango, R. J., "Optimally Discretized Finite Elements for Boundary Layer Stresses in Composite Laminates," *AIAA Journal*, Vol. 21, No. 6, 1983, pp. 614–620.

[9]Raju, I. S., and Crews, J. H., Jr., "Interlaminar Stress Singularities at a Straight Free Edge in Composite Laminate," *Computers and Structures*, Vol. 14, No. 1–2, 1981, pp. 21–28.

[10]Whitcomb, J. D., Raju, I. S., and Goree, J. G., "Reliability of the Finite Element Method for Calculating Free Edge Stresses in Composite Laminates," *Computers and Structures*, Vol. 15, No. 1, 1982, pp. 23–37.

[11]Giavotto, V., Borri, M., Mantegazza, P., Ghiringhelli, G. L., Caramaschi, V., Maffioli, G. C., and Mussi, F., "Anisotropic Beam Theory and Applications," *Computers and Structures*, Vol. 16, No. 1–4, 1983, pp. 403–413.

[12]Wang, S. S., and Yuan, F. G., "A Hybrid Finite Element Approach to Composite Laminate Elasticity Problems with Singularities," *Journal of Applied Mechanics*, Vol. 50, Dec. 1983, pp. 835–844.

[13]Tang, S., "A Boundary Layer Theory—Part I. Laminated Composites in Plane Stress," *Journal of Composite Materials*, Vol. 9, Jan. 1975, pp. 33–41.

[14]Tang, S., and Levy, A., "A Boundary Layer Theory—Part II. Extension of Laminated Finite Strip," *Journal of Composite Materials*, Vol. 9, Jan. 1975, pp. 42–52.

[15]Hsu, P. W., and Herakovich, C. T., "Edge Effect in Angle-Ply Composite Laminates," *Journal of Composite Materials*, Vol. 11, Jan. 1977, pp. 422–428.

[16]Wang, J. T. S., and Dickson, J. N., "Interlaminar Stresses in Symmetric Composite Laminates," *Journal of Composite Materials*, Vol. 12, Oct. 1978, pp. 390–402.

[17]Pipes, R. B., and Pagano, N. J., "Interlaminar Stresses in Composite Laminates—An Approximate Elasticity Solution," *Journal of Applied Mechanics*, Vol. 41, Sept. 1974, pp. 668–672.

[18]Wang, S. S., and Choi, I., "Boundary-Layer Effects in Composite Laminates: Part 1—Free Edge Stress Singularities," *Journal of Applied Mechanics*, Vol. 49, Sept. 1982, pp. 541–548.

[19]Wang, S. S., and Choi, I., "Boundary-Layer Effects in Composite Laminates: Part 2—Free Edge Stress Solutions and Basic Characteristics," *Journal of Applied Mechanics*, Vol. 49, Sept. 1982, pp. 549–560.

[20]Pagano, N. J., "Stress Fields in Composite Laminates," *International Journal of Solids and Structures*, Vol. 14, No. 5, 1978, pp. 385–400.

[21]Pagano, N. J., "Free Edge Stress Fields in Composite Laminates," *International Journal of Solids and Structures*, Vol. 14, No. 5, 1978, pp. 401–406.

[22]Kassapoglou, C., and Lagace, P. A., "An Efficient Method for the Calculation of Interlaminar Stresses in Composite Materials," *Journal of Applied Mechanics*, Vol. 53, Dec. 1986, pp. 744–750.

[23]Lin, C. C., Hsu, C. Y., and Ko, C. C., "Interlaminar Stresses in General Laminates with Straight Free Edges," *AIAA Journal*, Vol. 33, No. 8, 1995, pp. 1471–1476.

[24]Davì, G., and Milazzo, A., "Stress Fields in Composite Cross-Ply Laminates," *Proceedings of the 11th International Conference on Boundary Element Technology*, Computational Mechanics Publications, Southampton, England, U.K., 1996, pp. 175–183.

[25]Davì, G., "Stress Fields in General Composite Laminates," *AIAA Journal*, Vol. 34, No. 12, 1996, pp. 2604–2608.

[26]Davì, G., and Milazzo, A., "Boundary Element Solution for the Free Edge Stresses in Composite Laminates," *Journal of Applied Mechanics*, Vol. 64, No. 4, 1997, pp. 877–884.

[27]Ye, L., "Some Characteristics of Distributions of Free-Edge Interlaminar Stresses in Composite Laminates," *International Journal of Solids and Structures*, Vol. 26, No. 3, 1990, pp. 331–351.

[28]Chan, W. S., and Ochoa, O. O., "An Integrated Finite Element Model of Edge-Delamination Analysis due to a Tension, Bending and Torsion Load," AIAA Paper 87-0704, April 1987.

[29]Chan, W. S., and Ochoa, O. O., "Delamination Characterization of Laminates Under Tension, Bending and Torsion Loads," *Computational Mechanics*, Vol. 6, No. 4, 1990, pp. 393–405.

[30]Yin, W. L., "Free Edge Effects in Anisotropic Laminates Under Extension, Bending and Twisting. Part 1—A Stress Function Based Variational Approach," *Journal of Applied Mechanics*, Vol. 61, June 1994, pp. 410–415.

[31]Yin, W. L., "Free Edge Effects in Anisotropic Laminates Under Extension, Bending and Twisting. Part 2—Eigenfunction Analysis and the Results for Symmetric Laminates," *Journal of Applied Mechanics*, Vol. 61, June 1994, pp. 416–421.

[32]Murthy, P. L. N., and Chamis, C. C., "Free-Edge Delamination: Laminate Width and Loading Conditions Effects," *Journal of Composites Technology and Research*, Vol. 11, No. 1, 1989, pp. 15–22.

[33]Davì, G., and Milazzo, A., "Bending Stress Fields in Composite Laminate Beams by Boundary Integral Formulation," *Computers and Structures*, Vol. 71, No. 3, 1999, pp. 267–276.

[34]Davì, G., and Milazzo, A., "Boundary Integral Formulation for Composite Laminates in Torsion," *AIAA Journal*, Vol. 35, No. 10, 1997, pp. 1660–1666.

[35]Leger, C. A., and Chan, W. S., "Analysis of Interlaminar Stresses in Symmetric and Unsymmetric Laminates Under Various Loadings," AIAA Paper 93-1511, April 1993.

[36]Kassapoglou, C., "Determination of Interlaminar Stresses in Composite Laminates Under Combined Loads," *Journal of Reinforced Plastics and Composites*, Vol. 9, Jan. 1990, pp. 33–58.

[37]Kim, T., and Atluri, S. N., "Interlaminar Stresses in Composite Laminates Under Out-of-Plane Shear/Bending," *AIAA Journal*, Vol. 32, No. 8, 1994, pp. 1700–1708.

[38]Davì, G., "General Theory for Cross-Ply Laminated Beams," *AIAA Journal*, Vol. 35, No. 8, 1997, pp. 1334–1340.

[39]Lekhnitskii, S. G., *Theory of Elasticity of an Anisotropic Body*, Holden-Day, San Francisco, 1963.

[40]Kayupov, M. A., and Kuriyagawa, M., "Stress and Displacement Discontinuity Boundary Elements in an Anisotropic Medium," *Proceedings of the 11th International Conference on Boundary Element Technology*, Computational Mechanics Publications, Southampton, England, U.K., 1996, pp. 193–202.

[41]Mantic, V., and Paris, F., "Symmetrical Representation of Stresses in the Stroh Formalism and Its Application to a Dislocation and a Dislocation Dipole in an Anisotropic Medium," *Journal of Elasticity*, Vol. 47, No. 2, 1997, pp. 101–120.

E. R. Johnson
*Associate Editor*